

Three-dimensional printing with sacrificial materials for soft matter manufacturing

Christopher S. O'Bryan, Tapomoy Bhattacharjee, Sean R. Niemi, Sidhika Balachandar, Nicholas Baldwin, S. Tori Ellison, Curtis R. Taylor, W. Gregory Sawyer, and Thomas E. Angelini

Rheological concepts

Jammed granular particles,¹⁻⁵ entangled polymer solutions,⁶ micelles packed into solid-like phases,^{7,8} and polymer networks with reversible bonds^{9,10} are among the materials that have been investigated for the manufacture of soft structures. These different categories of soft matter exhibit unique and complex frequency-dependent behaviors, however, they are often described by classical viscoelastic models within bounded frequency ranges. While simple classical models do not perfectly capture the complex behavior of these materials, they can provide a framework for predicting performance in three-dimensional (3D) printing applications. The two simplest frameworks for describing the rheology of viscoelastic materials are the Maxwell and Kelvin–Voigt models.¹¹⁻¹⁴

Maxwell materials:

Low-frequency fluids/high-frequency solids

Soft matter printing materials that behave like solids at high frequencies and liquids at low frequencies may be described by the Maxwell model (Figure S1a). Even in the limit of zero applied stress and zero strain, these materials are fluids over long time scales and are often referred to as “Maxwell fluids.” The stress relaxation curve of these materials is modeled by a spring and dashpot arranged in series, given by $G(t) = G_0 e^{-t/\tau}$, where $G(t)$ is the ratio of stress to strain as a function of time, often called the stress relaxation modulus. The frequency-dependent elastic shear modulus (G') and viscous shear modulus (G'') of Maxwell materials can be obtained by Fourier transforming the stress relaxation curve and are given by:

$$G'(\omega) = G_0 \frac{(\omega\tau)^2}{1 + (\omega\tau)^2} \quad \text{and} \quad G''(\omega) = G_0 \frac{(\omega\tau)}{1 + (\omega\tau)^2}, \quad (1)$$

where G_0 is the high-frequency elastic modulus, ω is the frequency, and τ is the characteristic structural relaxation time. Generally, materials exhibiting thermally driven relaxations,

including spontaneous bond-breaking, particle rearrangements, or polymer entanglements, will behave like Maxwell fluids at long time scales. In soft matter 3D printing, materials that appear to behave like Maxwell fluids at low frequencies include concentrated micelles^{15,16} and polymer networks with weak reversible bonds.^{9,10} Micelles have a counterintuitive pairing of structure and rheology; they exhibit fluid-like behavior at low frequencies even when concentrated into packings with crystalline symmetry.^{15,16}

Kelvin–Voigt materials:

Low-frequency solids/high-frequency fluids

In direct contrast to Maxwell fluids, soft matter printing materials that exhibit elastic behavior at low frequencies and viscous behavior at high frequencies may be described by the Kelvin–Voigt model (Figure S1b). In the Kelvin–Voigt model, the elastic and viscous shear moduli are given by $G'(\omega) = G$ and $G''(\omega) = \eta\omega$, where G is a frequency independent shear modulus and η is a simple Newtonian viscosity. These moduli can be obtained by Fourier transforming the stress relaxation curve of a spring and dashpot in parallel.^{11,12} The Kelvin–Voigt model captures the elastic modulus of soft materials that do not spontaneously restructure under thermal forces, such as covalently cross-linked hydrogels or soft jammed granules (particle diameter larger than 1 μm). However, these materials generally exhibit non-Newtonian dissipation, so the model's G'' scaling law often fails to describe material behavior. In soft matter printing, jammed granular microgels have been shown to exhibit the frequency-independent elastic modulus of the Kelvin–Voigt model and behave dominantly like elastic solids, even in the low-frequency limit.^{1,3,4,17,18}

Applying rheological models to soft matter printing materials

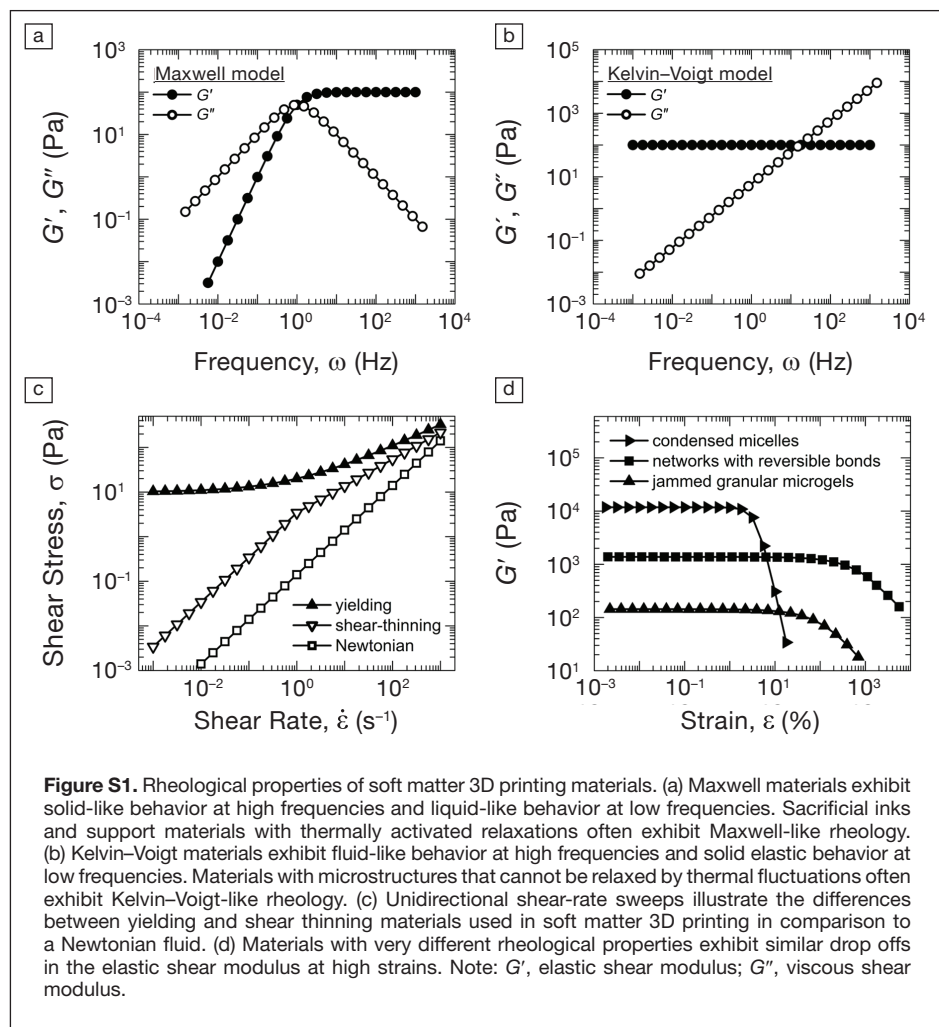
The dramatically different low-frequency behaviors of these two classes of material are reflected in their responses to applied strain in the zero-frequency limit. The zero-frequency

Christopher S. O'Bryan, Department of Mechanical and Aerospace Engineering, University of Florida, USA; csobryan@ufl.edu
 Tapomoy Bhattacharjee, Department of Mechanical and Aerospace Engineering, University of Florida, USA; tapomoy@ufl.edu
 Sean R. Niemi, Department of Mechanical and Aerospace Engineering, University of Florida, USA; impstar@ufl.edu
 Sidhika Balachandar, University of Florida, USA; sbalachandar@gm.sbac.edu
 Nicholas Baldwin, University of Florida, USA; nbaldwin98@ufl.edu
 S. Tori Ellison, Department of Mechanical and Aerospace Engineering, University of Florida, USA; tr Ellison@ufl.edu
 Curtis R. Taylor, Department of Mechanical and Aerospace Engineering, University of Florida, USA; curtis.taylor@ufl.edu
 W. Gregory Sawyer, Department of Mechanical and Aerospace Engineering, University of Florida, USA; wgsawyer@ad.ufl.edu
 Thomas E. Angelini, Department of Mechanical and Aerospace Engineering, University of Florida, USA; t.e.angelini@ufl.edu

limit can be probed by performing unidirectional shear-rate sweeps in which stress is measured as a function of shear rate (Figure S1c). For example, at low shear rates, jammed granular microgels bear shear-rate-independent stresses and are dominated by elasticity; at high shear rates, these materials fluidize and are dominated by viscous losses.^{17,19} This behavior is captured by $\sigma = \sigma_y + k\dot{\epsilon}^p$ where σ is the shear stress, σ_y is the yield stress of the material, $\dot{\epsilon}$ is the shear rate, and p is a dimensionless constant; $p = 1$ corresponds to a Bingham plastic and $p < 1$ corresponds to a Herschel–Bulkley material.^{17,20,21} In contrast, materials well described by the Maxwell model, including polymer melts, entangled polymer solutions, polymer networks with reversible bonds, and concentrated micelles, are dominantly fluid-like at low frequencies, and therefore, do not exhibit a shear-rate-independent shear stress at low shear rates.^{10,22} Shear-rate

sweeps on several of these materials reveal shear-thinning behavior, in which stress scales as $\dot{\epsilon}$ at low shear rates and $\dot{\epsilon}^p$ at high shear rates, where $p < 1$ (Figure S1c).

In the published literature, when new materials and methods for soft matter printing applications are reported, the yielding of a material is often characterized by measuring how the elastic shear modulus, G' , varies with applied stress or strain at a single oscillatory frequency. In these tests, G' is most always found to be a constant at low levels of stress or strain and to drop dramatically at high stresses or strains. The threshold stress at which the elastic shear modulus begins to drop is used to approximate a yield stress. Most complex fluids, including jammed granular materials, colloidal glasses, concentrated polymer solutions, polymer melts, and polymer networks with reversible bonds, exhibit this transition (Figure S1d). The preceding discussions of Maxwell fluids, Kelvin–Voigt solids, yielding, and shear thinning, demonstrate that the underlying mechanisms controlling this general “thinning” behavior can differ significantly from material to material. Thus, caution must be taken when interpreting measurements of G' versus stress or strain; the performance of a material



in 3D printing applications are not easily inferred from such measurements. A more tractable characterization is attained from measuring frequency-dependent moduli and stress as a function of shear rate.

Methods

All literary searches conducted for this review were performed in Google Scholar using combinations of the following search terms: 3D printing, 3D bioprinting, biofabrication, soft matter printing, hydrogel printing, embedded printing, direct write, sacrificial material, sacrificial support, sacrificial scaffold, sacrificial inks, biomaterials, self-healing, granular materials, yield stress materials, liquid like solids, tissue engineering, rheology. All graphical representations of data presented here were developed specifically for this review article by the authors using data gathered during literary searches; citations are included for the sources of the presented data in the figure and figure captions as appropriate.

All papers that contain the necessary data related to printed feature size, material deposition rate, and tangential velocity of the nozzle were included in Figures 2 and 3 (in the main

article). When presented in the text or in a tabular format, the material deposition rates, feature sizes, and tangential velocities were copied directly; when presented in a graphical format, these variables were measured from the given axes or scale bars. The cross-sectional area of printed structures was determined using $A = \pi ab/4$, where a is the width and b is the height of the printed structure. When only a single dimension was given, the cross-sectional area was approximated by $A = \pi d^2/4$. Those papers that did not provide sufficient information to determine one or more of the required variables were excluded from Figures 2 and 3 (in the main article).

References

1. T. Bhattacharjee, S.M. Zehnder, K.G. Rowe, S. Jain, R.M. Nixon, W.G. Sawyer, T.E. Angelini, *Sci. Adv.* **1**, e1500655 (2015).
2. T.J. Hinton, A. Hudson, K. Pusch, A. Lee, A.W. Feinberg, *ACS Biomater. Sci. Eng.* **2**, 1781 (2016).
3. C.S. O'Bryan, T. Bhattacharjee, S. Hart, C.P. Kabb, K.D. Schulze, I. Chilakala, B.S. Sumerlin, W.G. Sawyer, T.E. Angelini, *Sci. Adv.* **3**, e1602800 (2017).
4. T. Bhattacharjee, C.J. Gil, S.L. Marshall, J.M. Urueña, C.S. O'Bryan, M. Carstens, B. Keselowsky, G.D. Palmer, S. Ghivizzani, C.P. Gibbs, *ACS Biomater. Sci. Eng.* **2**, 1787 (2016).
5. Y. Jin, A. Compaan, T. Bhattacharjee, Y. Huang, *Biofabrication* **8**, 025016 (2016).
6. J.N. Hanson Shepherd, S.T. Parker, R.F. Shepherd, M.U. Gillette, J.A. Lewis, R.G. Nuzzo, *Adv. Funct. Mater.* **21**, 47 (2011).
7. K.A. Homan, D.B. Kolesky, M.A. Skylar-Scott, J. Herrmann, H. Obuobi, A. Moisan, J.A. Lewis, *Sci. Rep.* **6**, 34845 (2016).
8. D.B. Kolesky, R.L. Truby, A. Gladman, T.A. Busbee, K.A. Homan, J.A. Lewis, *Adv. Mater.* **26**, 3124 (2014).
9. C.B. Highley, C.B. Rodell, J.A. Burdick, *Adv. Mater.* **27**, 5075 (2015).
10. C.B. Rodell, A.L. Kaminski, J.A. Burdick, *Biomacromolecules* **14**, 4125 (2013).
11. F.F. Ling, W.M. Lai, D.A. Lucca, *Fundamentals of Surface Mechanics: With Applications* (Springer, New York, 2012).
12. L.E. Malvern, *Introduction to the Mechanics of a Continuous Medium* (Prentice-Hall, Englewood Cliffs, NJ, 1969).
13. J.C. Maxwell, *Philos. Trans. R. Soc. Lond.* **157**, 49 (1867).
14. M. Rubinstein, R.H. Colby, *Polymer Physics* (Oxford University, New York, 2003).
15. J.-P. Habas, E. Pavie, A. Lapp, J. Peyrelasse, *J. Rheol.* **48**, 1 (2004).
16. C. Perreur, J.-P. Habas, J. Peyrelasse, J. François, A. Lapp, *Phys. Rev. E Stat. Nonlin. Soft Matter Phys.* **63**, 031505 (2001).
17. C.J. Dimitriou, R.H. Ewoldt, G.H. McKinley, *J. Rheol.* **57**, 27 (2013).
18. K.J. LeBlanc, S.R. Niemi, A.I. Bennett, K.L. Harris, K.D. Schulze, W.G. Sawyer, C. Taylor, T.E. Angelini, *ACS Biomater. Sci. Eng.* **2**, 1796 (2016).
19. P. Menuet, S. Seiffert, J. Sprakel, D.A. Weitz, *Soft Matter* **8**, 156 (2012).
20. E.C. Bingham, *Fluidity and Plasticity* (McGraw-Hill, New York, 1922).
21. W. Herschel, R. Bulkley, *Proc. Am. Soc. Test. Mater.* (1926), pp. 621–633.
22. E. Eiser, F. Molino, G. Porte, X. Pithon, *Rheol. Acta* **39**, 201 (2000). □